frontiers | Frontiers in Plant Science

TYPE Original Research
PUBLISHED 19 October 2022
DOI 10.3389/fpls.2022.1049114

OPEN ACCESS

EDITED BY
Qiusheng Kong,
Huazhong Agricultural University, China

REVIEWED BY
Shi Liu,
Northeast Agricultural University, China
Tongkun Liu,
Nanjing Agricultural University, China

*CORRESPONDENCE
Dexi Sun
sundexi@caas.cn
Junpu Liu
liujunpu@caas.cn

†These authors have contributed equally to this work

SPECIALTY SECTION
This article was submitted to Plant Bioinformatics, a section of the journal Frontiers in Plant Science

RECEIVED 20 September 2022
ACCEPTED 28 September 2022
PUBLISHED 19 October 2022

CITATION
Zhu Y, Yuan G, Wang Y, An G, Li W, Liu J and Sun D (2022) Mapping and functional verification of leaf yellowing genes in watermelon during whole growth period.
Front. Plant Sci. 13:1049114.
doi: 10.3389/fpls.2022.1049114

Mapping and functional verification of leaf yellowing genes in watermelon during whole growth period

Yingchun Zhu[1,2†], Gaopeng Yuan[1†], Yifan Wang[1], Guolin An[1], Weihua Li[1], Junpu Liu[1,2*] and Dexi Sun[1*]

[1]The Key Laboratory of Genetic Resource Evaluation and Application of Horticultural Crops (Fruit), Ministry of Agriculture, Zhengzhou Fruit Research Institute, Chinese Academy of Agricultural Sciences, Zhengzhou, China, [2]Western Research Institute, Chinese Academy of Agricultural Sciences, Changji, China

Increasing light energy utilization efficiency is an effective way to increase yield and improve quality of watermelon. Leaf is the main place for photosynthesis, and the color of leaf is directly related to the change of photosynthesis. In addition, leaf yellowing can be used as a marker trait to play an important role in watermelon hybrid breeding and improve seed breeding. It can not only be used to eliminate hybrids at seedling stage, but also be used to determine seed purity. In this study, transcriptome analysis was first carried out using the whole growth period leaf yellowing watermelon mutant *w-yl* and inbred line ZK, and identified 2,471 differentially expressed genes (DEGs) in the comparison group *w-yl*-vs-ZK. Among the top 20 terms of the gene ontology (GO) enrichment pathway, 17 terms were related to photosynthesis. KEGG pathway enrichment analysis showed that the most abundant pathway was photosynthesis—antenna proteins. The F_2 population was constructed by conventional hybridization with the inbred line ZK. Genetic analysis showed that leaf yellowing of the mutant was controlled by a single recessive gene. The leaf yellowing gene of watermelon located between Ind14,179,011 and InD16,396,362 on chromosome 2 by using indel-specific PCR markers, with a region of 2.217 Mb. In the interval, it was found that five genes may have gene fragment deletion in *w-yl*, among which *Cla97C02G036010*, *Cla97C02G036030*, *Cla97C02G036040*, *Cla97C02G036050* were the whole fragment loss, and *Cla97C02G0360* was the C-terminal partial base loss. Gene function verification results showed that *Cla97C02G036040*, *Cla97C02G036050* and *Cla97C02G036060* may be the key factors leading to yellowing of *w-yl* leaves.

KEYWORDS

Watermelon, leaf yellowing, gene mapping, fragment deletion, gene function

Introduction

Photosynthesis is essential in the process of plant growth and development, which is of great significance for plant survival. Leaves are the main place for photosynthesis in plants, and leaf color determines photosynthetic efficiency to a large extent (Chen et al., 2022). Different pigments can absorb light waves of different lengths, so leaves of plants show different colors due to different pigment contents and proportions. Leaf color mutation is a frequent and easily recognized phenomenon in nature, so leaf color mutants are ideal materials for studying plant development (Yuan et al., 2022b). At present, mutant materials have been found in a variety of plants, and the leaf color mutation types include albino, etiolation, stripe, yellow-green, green-yellow, green-white, light green and verdant green, etc (Awan et al., 1980). There are many ways of forming leaf color mutation. External factors mainly include light, temperature, plant hormones, mineral elements and metal ions. Internal factors mainly include genes related to photosynthetic pigment metabolism pathway, such as chloroplast biosynthesis pathway, chlorophyll degradation pathway, heme metabolism pathway and carotenoid metabolism pathway; as well as genes related to chloroplast development, such as chloroplast development and protein synthesis, nucleoplasmic interactions. All of these can lead to a decrease in the chlorophyll content of plant leaves, resulting in the leaves can not appear green color (Zhang et al., 2006; Sugliani et al., 2016; Li et al., 2018).

Studies on leaf color mutations mainly focus on the cell structure, photosynthetic physiology, molecular biology and other aspects of leaf color mutants, among which more in-depth studies have been conducted in model plants such as rice and *Arabidopsis*. For example, more than 160 leaf color mutants have been found in rice, distributed on 12 chromosomes, among which a small number of leaf color mutants have been cloned (Dong et al., 2013; Huang et al., 2017; Tan et al., 2019). Among them, 14 genes are directly involved in chlorophyll biosynthesis and catabolism (Sakuraba et al., 2013), and 6 genes are indirectly involved in this process (Yang et al., 2011), while 16 genes are directly involved in chloroplast development regulation (Gothandam et al., 2005) and 3 were indirectly involved in this process (Hibara et al., 2009) Therefore, the mutant genes are mainly divided into two categories, namely, genes in the chlorophyll biosynthesis and degradation pathway and genes in the chloroplast development pathway. In addition, previous studies have proved that most leaf color mutations are nuclear inheritance except for a small number of leaf color mutations for cytoplasmic inheritance (Kong et al., 2016; Li et al., 2021a; Li et al., 2021b). In recent years, with the application of high-throughput sequencing, the study of leaf color mutation has been gradually carried out in some important economic crops and ornamental plants, such as tea, pepper, maize, melon and cucumber (Shao et al., 2013; Li, 2016; Lai et al., 2018; Wang et al., 2019; Zhu et al., 2019; Gao et al., 2020; Xiong et al., 2020), which will help improve crop quality and increase yield (Shao, 2013; Ren et al., 2019). The results of the latest study on cucumber showed that the post-green mutant *SC311Y* was controlled by a recessive gene, which was identified as the gene controlling chloroplast development by BSA-seq and RNA-seq techniques (Zhang et al., 2022).

The genetic basis of watermelon is narrow and the natural mutation rate is low. There are few studies on watermelon leaf color mutants. The leaf color mutation materials are mainly divided into four categories: (1) watermelon leaf color mottled mutants, which are characterized by white-green cotyledons and mosaic-like spots in the first true leaf under low temperature environment (Provvidenti, 1994; Wang et al., 2011); (2) watermelon albino mutant, showing pale yellow or pale cream cotyledons, gradually turning green but remaining white at leaf margins, white tendrils, petioles, petals and hypocotyls (Zhang et al., 1996; Wang et al., 2011; Hou et al., 2016); (3) incomplete dominant yellow leaf mutants (Hou et al., 2016); (4) In post-green mutants, the leaves showed light green cotyledons and leaves at the early stage, and changed to normal green at the later stage (Wang and Wang, 1997; Ma and Zhang, 1999; Wang et al., 2011; Xu et al., 2022). In terms of genetic analysis and molecular biology, the early stage mainly focused on the study of genetic patterns, and confirmed that watermelon leaf color mutants were controlled by recessive genes based on the discovered mutant materials (Rhodes, 1986; Provvidenti, 1994; Zhang et al., 1996). With the publication of watermelon genome and the rapid development of sequencing technology (Guo et al., 2019; Wu et al., 2019), more high density genetic maps of watermelon emerged (Duan et al., 2022), but only a few maps involved watermelon leaf color. For example, Haileslassie (Haileslassie, 2020) found the presence of a SNP in the gene *ClCG03G010030* of the watermelon post-green mutant *Houlv*, resulting in an arginine to lysine mutation. The gene encodes an FtsH extracellular protease family protein which is involved in the development of early chloroplast. Exploring the mechanism of leaf color variation can provide a theoretical basis for genetic improvement and meet people's needs in production, seed selection and breeding.

China is the largest watermelon planting and consumption country in the world. Although the demands for watermelon is diversified, cultivating new varieties with high yield and high quality is still the main direction of watermelon breeding. Improving the utilization efficiency of light energy of watermelons is an effective way to promote yield and improve quality. In this study, yellow leaf throughout the whole growth period material *w-yl* and green leaf material ZK were used as experimental materials. The position of the leaf yellowing gene in the chromosome was preliminarily located by BSA-seq technology. The high-density genetic map was constructed by the F_2 population using InDel markers for mapping the position of the mutant gene in the chromosome, and the key candidate

genes and key variations were screened in combination with transcriptome data. Finally, the virus-induced gene silencing (VIGS) assay was performed on the key candidate genes to clarify the function of the yellowing leaf gene. The development of this study will help to explore the mechanism of leaf yellowing in the whole growth period of watermelon, and provide theoretical support for the application of leaf yellowing and molecular marker-assisted selection of new watermelon varieties with high photosynthetic efficiency.

Materials and methods

Plant material cultivation and samples collection

The leaf color yellowing mutant material *w-yl* was obtained from the National Mid-term Genebank for Watermelon and Melon (Zhengzhou, China), the leaves in the whole growth period were yellow, including cotyledon and fruit. Normal green leaf material ZK was supplied by the Diploid Watermelon Genetics and Breeding Research Group of Zhengzhou Fruit Research Institute (ZZFRI) of Chinese Academy of Agricultural Sciences (CAAS). In this study, the mutant material was crossed with the ZK, and six generations were constructed: P_1 (the yellow parent *w-yl*), P_2 (the green leaf parent ZK), F_1 (orthogonal), BC_1P_1, BC_1P_2, and F_2. The materials were planted in a greenhouse at the Xinxiang Comprehensive Experimental Base of CAAS, with a row spacing of 1.5 m and a plant spacing of 0.4 m. The phenotype of leaf color was determined by visual observation.

Plant for chlorophyll were planted in an artificial climate chamber and treated with different environmental factors at three true-leaf stage: temperature 35°C/28°C, light intensity 30,000 Lx, namely HTHL(high temperature and high light); temperature 35°C/28°C, light intensity 12,000 Lx, namely as HTNL (high temperature and normal light); temperature 35°C/28°C, light intensity 5,000 Lx, marked as HTLL (high temperature and low light); temperature 28°C/25°C, light intensity 30,000 Lx, marked as NTHL (normal temperature and high light); temperature 28°C/25°C, light intensity 12,000 Lx, marked as NTNL (normal temperature and normal light); temperature 28°C/25°C, light intensity 5,000 Lx, marked as NTLL (normal temperature and low light); temperature 15°C/15°C, light intensity 30,000 Lx, marked as LTHL (low temperature and high light); temperature 15°C/15°C, light intensity 12,000 Lx, marked as LTNL (low temperature and normal light); 15°C/15°C, 5,000 Lx, labeled as LTLL (low temperature and low light). Light cycle was 16h/8h, humidity 80%. Each treatment set three replicates. Chlorophyll content was determined after 8 days of treatment.

Plant for chlorophyll precursors and transcriptome sequencing were grown in a smart greenhouse in ZZFRI of CAAS, the light cycle was 16h/8h, the temperature was 25°C/18°C and the light is natural light. The leaves were sampled after 8 days of treatment.

Determination of pigment content

The third true leaf from five seedlings was sampled and mixed, weighed 0.1 g and put into a 15 mL centrifuge tube respectively, added 10 mL of 96% ethanol, and soaked in dark environment until the leaves turned completely white (Yuan et al., 2017). The absorbance A665, A649 and A470 at 665 nm, 649 nm and 470 nm were determined by UV spectrophotometer (UV-2600I, Shimadzu, Kyoto, Japan). The concentrations of chlorophyll a (chla), chlorophyll b (chlb), total chlorophyll (chla+b) and carotenoids were calculated using 96% ethanol as blank control. The equations are as following:

$$Chla\left(mg\cdot L^{-1}\right) = 13.95 \times A_{665} - 6.88 \times A_{649}$$

$$Chlb\left(mg\cdot L^{-1}\right) = 24.96 \times A_{649} - 7.32 \times A_{665}$$

$$Chla+b\left(mg\cdot L^{-1}\right) = chla + chlb = 6.63 \times A_{665} + 18.08 \times A_{649}$$

$$Carotenoids\left(mg\cdot L^{-1}\right) = \left(1000 \times A_{470} - 2.05 \times Chla - 114.8 \times Chlb\right)/248$$

Chlorophyll content ($mg\cdot g^{-1}$ = (C × V)/(W × 1000). C represents chlorophyll content, V represents the total volume of extract (mL), and W represents leaf mass (g).

Determination of chlorophyll precursor

The contents of main chlorophyll precursor in the process of chlorophyll synthesis were measured, among which δ-aminolevulinic acid (ALA) was determined according to the method of Dei (Dei, 2010) and the molar concentration of ALA was calculated with a molar extinction coefficient of 7.2×10^4 $mol^{-1}\cdot cm^{-1}$at 535 nm. Relative contents of protoporphyrin IX (protoIX), Mg-protoporphyrin IX (Mg-proto IX), and pchlide were determined according to the method of Rebeiz (Rebeizjames et al., 1975) and Lee (Lee et al., 1992). The relative mass molar concentration of Mg-Proto IX is presented as F_{ex595}^{440} : fluorescence emission intensity at 595 nm under 440 nm excitation light. Proto IX (F_{ex633}^{440}) = $(F_{ex633}^{440} - 0.25 \times F_{ex622}^{440} - 0.24 \times F_{ex640}^{440})/0.95$;
$Pchlide\ (_{ex640}^{440})$ = $(F_{ex640}^{440} - 0.03 \times F_{ex633}^{440})/0.99$.

RNA sequencing

Leaves of five plants were selected as a sample from *w-yl* and ZK, with three biological replicates respectively. Total RNA was extracted using RNeasy Plant Mini Kit (Beijing Tiagen), following the manufacturer's instructions. Then RNA was reversely transcribed to cDNA, and the cDNA fragments were segmented by PCR. Finally, the double-stranded PCR product is thermally denatured to form single-stranded circular DNA, which is then formatted into a final library. The cDNA library was sequenced by BGISEQ-500 system (BGI-Shenzhen, China) with reads of 100bp in length.

The sequencing data were screened to obtain Clean reads, which were then mapped into the '97103' watermelon genome (http://cucurbitgenomics.org/organism/21) using Bowtie2. Gene expression levels were calculated using FPKM (million fragments per kilobase). Based on KEGG (http://www.genome.jp/kegg/) and GO (http://www.geneontology.org/) database for gene annotation and function assignment. Differentially expressed genes (DEGs) were set as gene fold change ≥2.00 and false discovery rate ≤0.001. Through GO enrichment and KEGG enrichment pathways, the significantly enriched metabolic pathways were screened and compared with the whole genome background. Functional classification of DEGs was performed according to GO and KEGG annotation results and official classification, and FDR ≤ 0.01 was set as significant enrichment.

QPCR validation and gene expression analysis

Total RNA was extracted by plant RNA kit (Huayue Yang Biotechnology Co., LTD.). A total of 1.0 μg of RNA was used for cDNA synthesis using the PrimeScript RT kit and gDNA Eraser (TaKaRa) according to the manufacturer's protocol. Primers were designed using NCBI online tools (https://www.ncbi.nlm.nih.gov/tools/primer-blast/), and synthesized by Sangon Biotech (Shanghai, China). All the primer sequences were shown in Supplementary Table 1. Quantitative real-time PCR reaction procedure and system were as described previously (Yuan et al., 2022a). All primers are shown in Supplementary Table S1. The $2^{-\Delta\Delta Ct}$ method was used to calculate relative gene expression values (Kenneth and Thomas, 2002).

BSA-seq analysis of the leaf yellowing genes

Leaf DNA of 30 individual plants with yellowed and green extreme phenotypes in F2 population were selected for the construction of two extreme sequencing mixed pools, and parental DNA was used to construct the parental pools for sequencing analysis. The depth of parental sequencing was 20×, and the depth of extremely mixed-pool sequencing was 30×. Sequencing was performed by Biomarker Technologies Co, LTD (Beijing, China) using Illumina HiSeq2000. The sequencing read length was 150 bp.

Raw reads were filtered to remove reads containing adapter, and reads containing >5% N and low-quality reads (the number of bases with quality value Q ≤ 10 accounted for more than 50% of the whole read) were used to obtain clean reads for subsequent analysis. Clean reads were mapped to the '97103' watermelon genome (http://cucurbitgenomics.org/organism/21) using BWA software. Then GATK (4.0.4.0) and SNPeff (4.3) were used to annotate the mutation sites, and single nucleotide polymorphisms (SNPs) and insertion-deletion polymorphisms (InDels) were identified.

The SNP-index algorithm was used to establish the target region to find the significant difference in genotype frequency between the pool, and Δ(SNP-index) was used for statistics. In this project, the DISTANCE method was used to fit the ΔSNP-index, and then the region above the threshold was selected as the region related to the trait according to the association threshold. The stronger association between SNP and trait, the closer Δ(SNP-index) to 1.

Functional analysis of key genes

Using the cDNA of green leaf ZK as template, specific primers were designed to amplify the CDS regions of *Cla97C02G036010*, *Cla97C02G036030*, *Cla97C02G036040*, *Cla97C02G036050* and *Cla97C02G036060*, and the primers were shown in Supplementary Table 1. BamHI (GGATCC) restriction sites were added to both ends of the primers and inserted into the cucumber green mottle mosaic virus (CGMMV) gene silencing vector PV190 by homologous recombination to construct virus-induced gene silencing (VIGS) vector. The dual vector was transformed into *Agrobacterium tumefaciens* GV3101.

Induction and inoculation of *A. tumefaciens* according to Liu (Liu, 2019) When watermelon seedlings were at cotyledon stage, the induced *A. tumefaciens* was injected from the back of watermelon cotyledon with 1 mL syringe. The blank control (Blank, B), water control (Water, W), medium control (YT medium, Y), blank vector control (PV190, P) and *PDS* gene positive control (PDS) were set up respectively. Three biological replicates were set up for each treatment. Two weeks after injection, leaf phenotype was observed, and samples were collected for ultrastructural analysis, chlorophyll content measurement and gene expression analysis.

Ultrastructural observation of chloroplast

The above-mentioned leaves with phenotype after *A. tumefaciens* were used as materials, fixed with 4% glutaraldehyde (configured with pH 7.2 phosphate buffer) overnight at 4°C, rinsed with phosphate buffer three times, fixed with 1% osmium tetroxide for 1 h, rinsed with phosphate buffer three times, dehydrated with 30%, 50%, 70%, 80%, 95%, 100% ethanol and acetone step by step for 5 min, and finally embedded with resin. After sectioning, they were stained with 2% uranyl acetate saturated alcohol and lead citrate for 15 min, and the chloroplast ultrastructure was observed under transmission electron microscope (HT7700, Hitachi, Japan).

Data statistical analysis

All data graphs were analyzed by Office 2016 software. Differences were analyzed by SPSS 18.0 software, and one-way ANOVA was used for statistical analysis, $p< 0.05$ ($n = 3$) was considered significant difference.

Results

Genetic characteristics analysis of yellowing leaf color

The leaves of *w-yl* showed yellow throughout the whole growth period (Figure 1A), and the color did not change with environmental changes, such as temperature and light intensity (Figure 1B). Under different temperature and light intensity, there were no significant differences in the contents of chla, chlb, chla+b and carotenoids.

In addition, phenotypic data showed that all F_1 plants appeared green leaves, indicating that the yellow mutation was recessive. For F_2 plants, among the 237 progeny in the summer of 2018, 178 plants had green leaves and 59 plants had yellow leaves; among the 993 progeny in spring of 2019, 730 had green leaves and 263 had yellow leaves (Table 1). The χ^2 test of green and yellow leaves in the two seasons showed that the separation pattern was consistent with the Mendelian separation ratio of 3:1 ($\chi^2 > \chi^2_{0.05} = 3.841$). Furthermore, for the backcross progeny BC_1P_1 and BC_1P_2, the yellow leaf plants were 29 and 0 respectively, indicating that the yellowing mutation of watermelon leaves conformed to the genetic pattern controlled by a single recessive nuclear gene, and green leaves were dominant to yellowing.

Genetic characteristics analysis of yellowing leaf color

Previous studies had demonstrated that there are significant differences in chlorophyll content and photosynthetic indicators (Ren et al., 2019). To further validate the difference, the chlorophyll precursors, including ALA, protoIX, Mg-ProtoIX and pchlide were analyzed (Figure 2). The results showed that the contents of four indexes detected in the *w-yl* were significantly lower than those in ZK, which explained the low chlorophyll content to a certain extent.

RNA-seq for the leaves of *w-yl* and ZK

A total of 6 samples were measured by RNA-seq, including 3 samples for *w-yl* and 3 samples for ZK, yielding an average of 6.06 Gb of data per sample. The average rate of genome alignment was 89.40%, and the average rate of gene set alignment was 65.81% (Figure 3A). For the comparison group *w-yl*-vs-ZK, a total of 19,261 genes were detected, and there were 18,323 shared genes, including 2,471 DEGs (Figure 3A), with 848 up-regulated DEGs and 1893 down-regulated DEGs (Figure 3B).

GO enrichment and KEGG pathway enrichment analyses were carried out to better understand the function of DEGs. For GO enrichment, 17 of the top 20 selected GO terms were related to photosynthesis process, including 4 terms related to photosystem, such as photosystem (GO:0009521), photosystem I (GO:0009522), Photosystem II (GO:0009523), light harvesting in photosystem I (GO:0009768); 4 terms involved in photosynthesis, such as photosynthesis (GO:0015979), photosynthetic membrane (GO:0034357), photosynthesis—light reaction (GO:0019684) and photosynthesis—light harvesting (GO:0009765); 6 terms involved in thylakoid, such as thylakoid (GO:0009579), thylakoid membrane (GO:0042651), chloroplast thylakoid (GO:0009534), chloroplast thylakoid membrane (GO:0009535), plastid thylakoid (GO:0031976) and plastid thylakoid membrane (GO:0055035); 3 terms relate to pigments, such as tetrapyrrole binding (GO:0046906), chlorophyll binding (GO:0016168) and protein-chromophore linkage (GO:0018298) (Figure 3C; Supplementary Table S2). These results showed that *w-yl* and ZK had significant differences in photosynthesis.

For KEGG pathway enrichment, the two most significant enrichment pathways of the top 20 pathways were photosynthesis—antenna proteins and plant—pathogen interaction (Figure 3D; Supplementary Table S3). Due to the importance of antenna protein for photosynthesis (Figure 4A), we focused on the analysis of antenna protein-related DEGs, and completely screened 16 DEGs that encoded antenna protein (Figure 4B). LHCI and LHCII, as important components of photosystem I complex and photosystem II complex, are composed of four and six small components, respectively. For LHCI, the number of DEGs that encoded LHCI Chl a/b binding protein 1 (Lhca1), Lhca2, Lhca3 and Lhca4 was 1, 2, 1 and 2, respectively. For LHCII, the number of DEGs that encoded LHCII Chl a/b binding protein 1 (Lhcb1), Lhcb2, Lhcb3, Lhcb4, Lhcb5 and Lhcb6 was 4, 1, 1, 2, 1 and 1, respectively. The expression levels of all the 16 DEGs in ZK were significantly higher than those of *w-yl*, and the fold change was between 2.6 and 14.0 (Figure 4B).

10.3389/fpls.2022.1049114

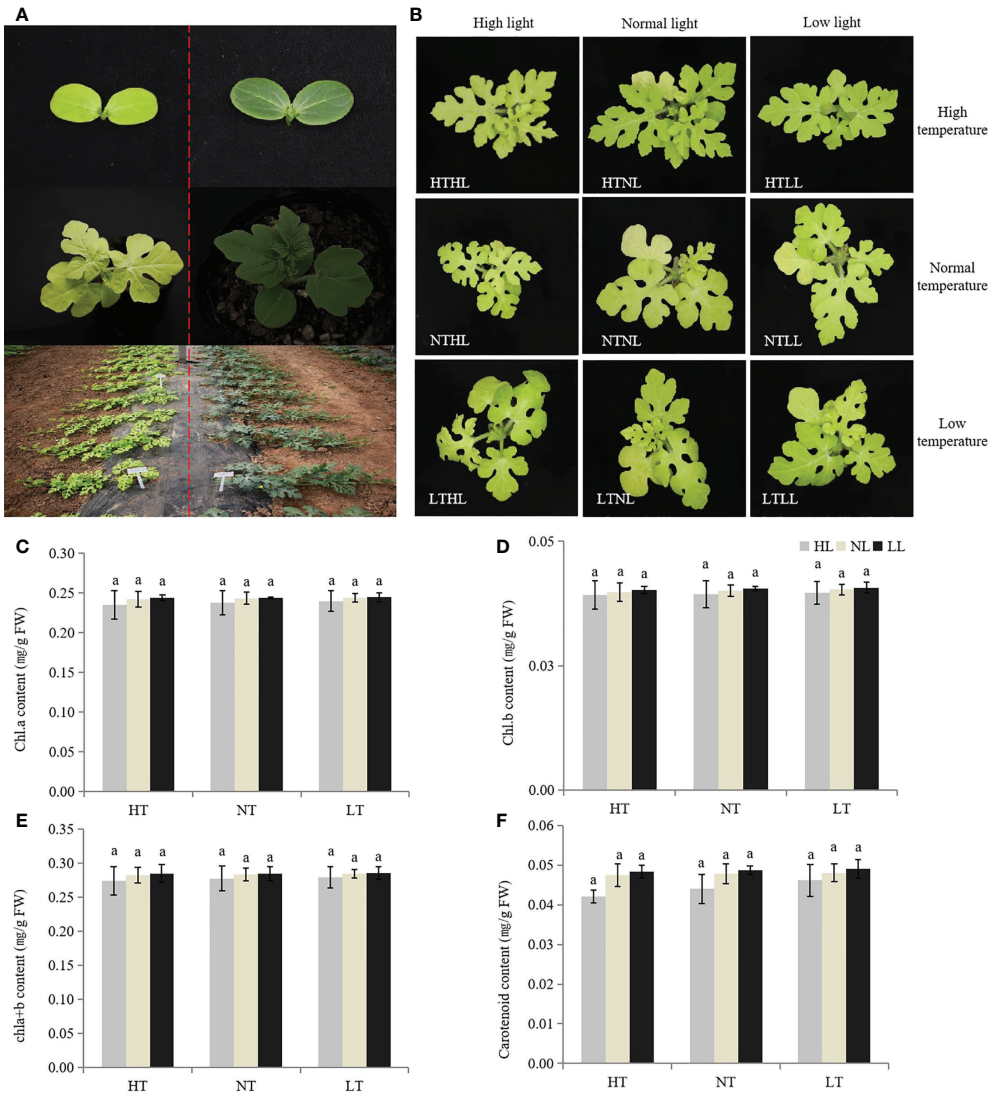

FIGURE 1
Plant phenotypes of w-yl and ZK. **(A)** Plant phenotypes of w-yl (left) and ZK (right) at different developmental stages. **(B)** Plant phenotypes of w-yl under different temperature and light intensity. The content of **(C)** chla, **(D)** chl b, **(E)** chla+b and **(F)** carotenoid under different temperature and light intensity. Small letters represent significant difference at P<0.05.

TABLE 1 Phenotype of yellow mutant to green leaf trait and Chi-square goodness-fit test ratios in different populations.

Population	Number	Green leaves	Yellow leaves	Expected ratio		P value
P_1	15		15			
P_2	15	15				
F_1	30	30				
F_2 (Summer of 2018)	237	178	59	3:1	0.0014	0.9701
F_2 (Spring of 2019)	993	730	263	3:1	1.1685	0.2797
BC_1P_1	54	29	25	1:1	0.2963	0.5862
BC_1P_2	30	30	0			

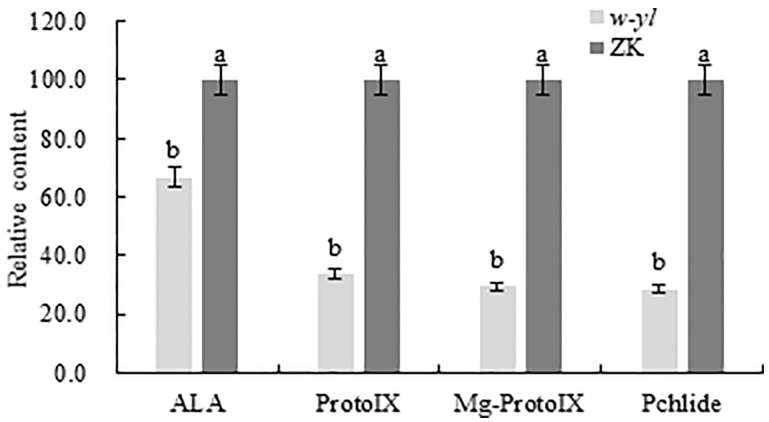

FIGURE 2
Chlorophyll precursors content of the *w-yl* and CK in pepper leaf. Small letters represent significant difference at P<0.05.

Verification of DEGs of qPCR and RNA-seq data

To verify the accuracy of RNA-seq data, 12 DEGs (*Cla97C02G035950*, *Cla97C02G035960*, *Cla97C02G035980*, *Cla97C02G036070*, *Cla97C02G036090*, *Cla97C02G036110*, *Cla97C02G036130*, *Cla97C02G036140*, *Cla97C02G036150*, *Cla97C02G036160*, *Cla97C02G036190* and *Cla97C02G036200*) of the 29 genes in the interval were selected to conduct qPCR (Figure 5). The results showed that expression patterns of 12 DEGs were highly consistent with those of genes in RNA-seq data, which demonstrated that the RNA-seq data are reliable.

Mapping of yellowing gene in w-yl leaf

In order to quickly identify the key candidate genes related to leaf color in the F_2 population, 30 green and 30 yellow leaf

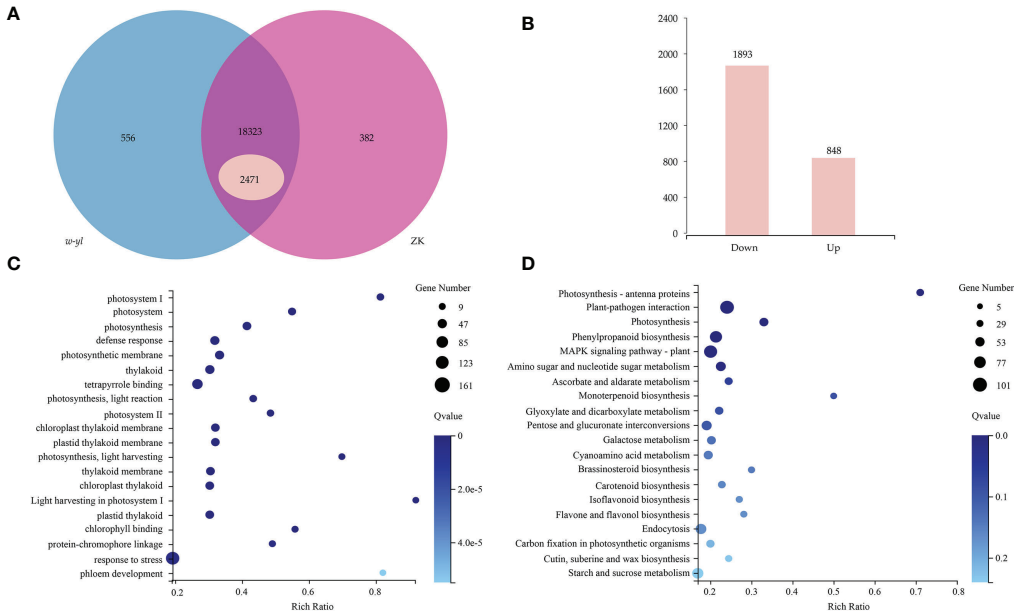

FIGURE 3
RNA-seq analysis for the leaves of *w-yl* and ZK. **(A)** Venn diagram of the relationship of *w-yl*-vs-ZK. **(B)** Number of up-regulated and down-regulated DEGs. **(C)** GO enrichment analysis of DEGs. **(D)** KEGG pathenrichment analysis of DEGs.

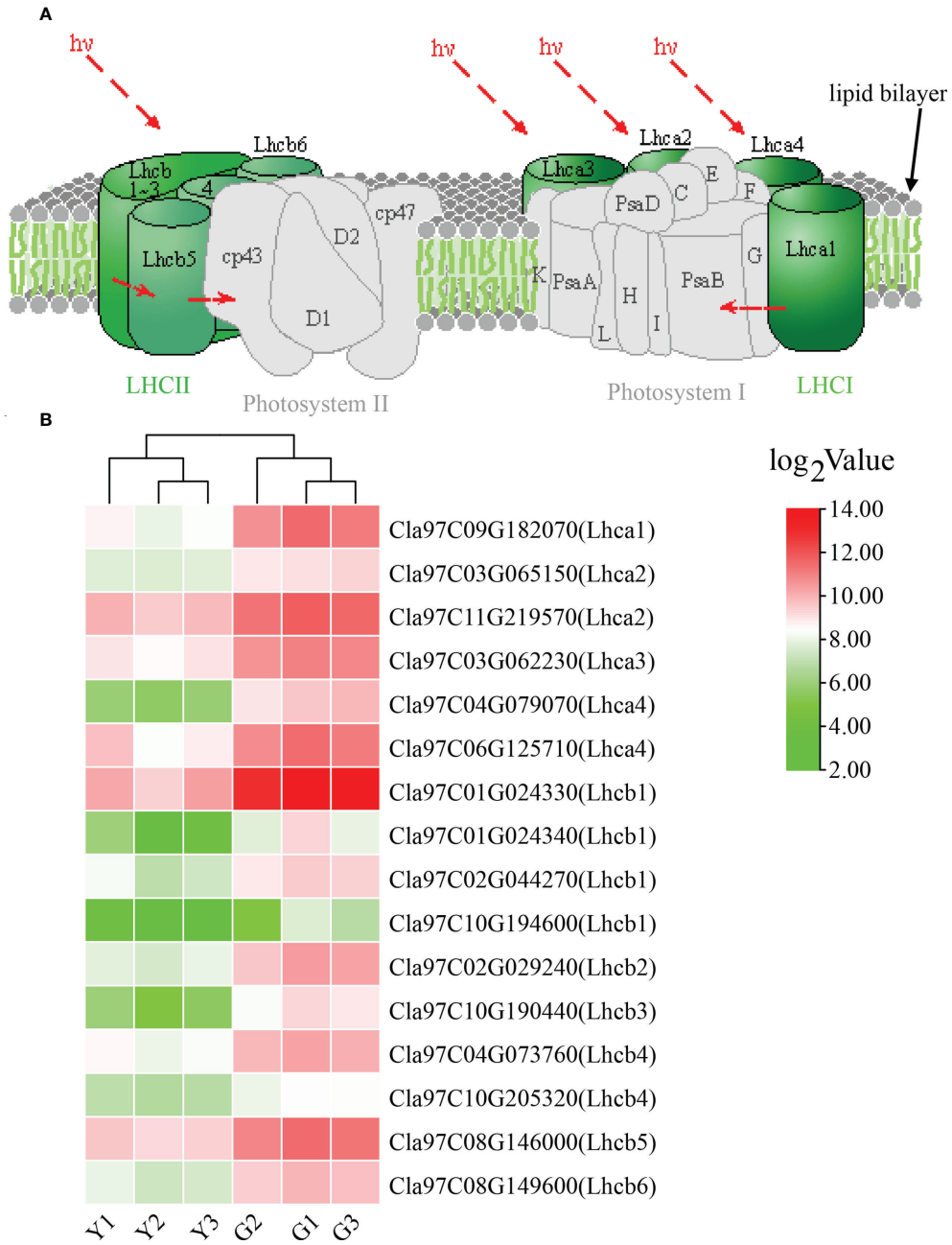

FIGURE 4
Analysis of the photosynthesis—antenna proteins. **(A)** Role of photosynthesis—antenna proteins in photosynthetic system. **(B)** Expression of photosynthesis—antenna proteins related DEGs.

progeny were selected and sequenced on the Illumina platform. A total of 51.0 Gb clean bases were generated with an average depth of about 26.5×. Finally, we identified 266,255 SNPs between *w-yl* and ZK, and 83,373 SNPs between the F_2 pools. According to the SNP-index values of *w-yl* and ZK, the Δ(SNP-index) value of approximately 7.42 Mb genome region (11,540,000-18,960,000) on chromosome 2 was greater than the threshold (Figure 6A). These results indicated that this region might contain the key gene of watermelon leaf yellow traits.

In order to further locate the candidate genes for yellowing leaf, the chromosome region of the variation between *w-yl* and ZK were analyzed. A total of 12 pairs of InDel molecular markers (Supplementary Table S4) were developed for the candidate region

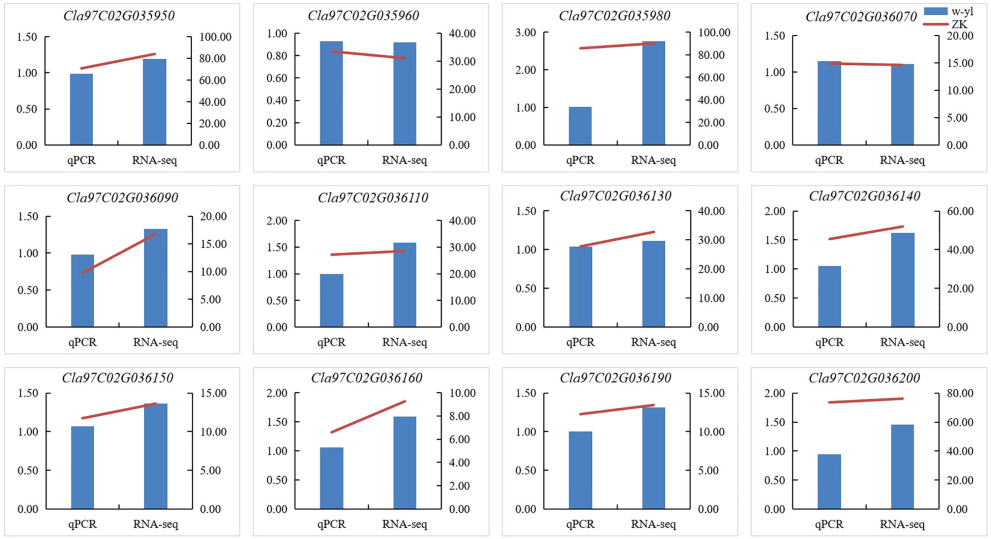

FIGURE 5
Verification of DEGs by RT-qPCR.

based on 233 F_2 populations. The results verified that these genes were in the range of 11.54 Mb—18.96 Mb on chromosome 2. Subsequently, based on the determination of leaf color phenotype data and individual exchange genotype, 12 recombinant individuals were further screened using 1883 F_2 populations. Finally, it is found that the candidate interval corresponds to the 2.217 Mb region of InD14,179,011—InD16,396,362 (Figure 6B). There were 29 genes in this region and annotated them according to the watermelon reference genome (Figure 3C; Table 2). Notably, compared with ZK, *Cla97C02G036010*, *Cla97C02G036020*, *Cla97C02G036030*, *Cla97C02G036040*, and *Cla97C02G036050* were completely absent in *w-yl*, and *Cla97C02G036060* had partial base deletion, suggesting that they were the key genes determining *w-yl* leaf color mutation (Supplementary Figure S1).

In addition, the results of agarose gel electrophoresis and qPCR showed that *Cla97C02G036010, Cla97C02G036020, Cla97C02G036030, Cla97C02G036040, Cla97C02G036050* and *Cla97C02G036060* could not be amplified in *w-yl*, as well as *Cla97C02G036020* also had no target product in ZK (Figure 7). The RNA-seq results also showed the same results (Figure 6C). These results further proved the importance of *Cla97C02G036010, Cla97C02G036030, Cla97C02G036040, Cla97C02G036050* and *Cla97C02G036060* in leaf yellowing.

Function analysis of yellowing gene in ZK leaf

In order to verify the gene function of the candidate genes, cucumber mosaic virus-mediated VIGS vector was used to perform gene silencing assay on ZK leaves. The results showed that at 16 days after inoculation (DAI), the plants inoculated with water (Figure 8B), medium (Figure 8C) and blank vector (Figure 8D) showed no significant difference in phenotype compared with the blank control (Figure 8A), while the positive control plants inoculated with *PDS* gene showed virus symptoms at DAI16, with severe true leaf pucking and chlorosis (Figure 8E). Watermelon plants silencing *Cla97C02G036010* (Figure 8F) and *Cla97C02G036030* (Figure 8G) showed symptoms of disease at DAI17, and their true leaves were slightly wrinkled and mottled greenish yellow. Watermelon plants silencing *Cla97C02G036040* (Figure 8H), *Cla97C02G036050* (Figure 8I) and *Cla97C02G036060* (Figure 8J) showed obvious virus symptoms at DAI13, with obvious true leaf wrinkling and large area mottled yellow.

Then the expression levels of the silenced genes were detected, when compared with the control group (B, W, Y, P and PDS), their expression levels were significantly reduced. Among them, the expression of *Cla97C02G030640* decreased most sharply, which were 2.9%, 2.9%, 2.8%, 3.2% and 27% of the control group, respectively (Figure 9). Besides, the results of chlorophyll content of leaves with phenotype showed that there was no significant difference in chla, chlb and chla+b content among groups B, W, Y and P, while the chlorophyll contents of silenced *PDS* group was significantly lower than that of the former four groups. For the five silenced genes, the contents of chla, chlb and chla+b were significantly lower than those of B, W, Y and P control groups. Among them, the contents of chla, chlb and chla+b in silenced genes *Cla97C02G030640* and *Cla97C02G030660* were the lowest and had not significantly different from those in silenced *PDS* group (Figure 10).

Furthermore, the ultrastructure of chloroplast was analyzed to analyze the reasons for these phenomenon. As a result, the

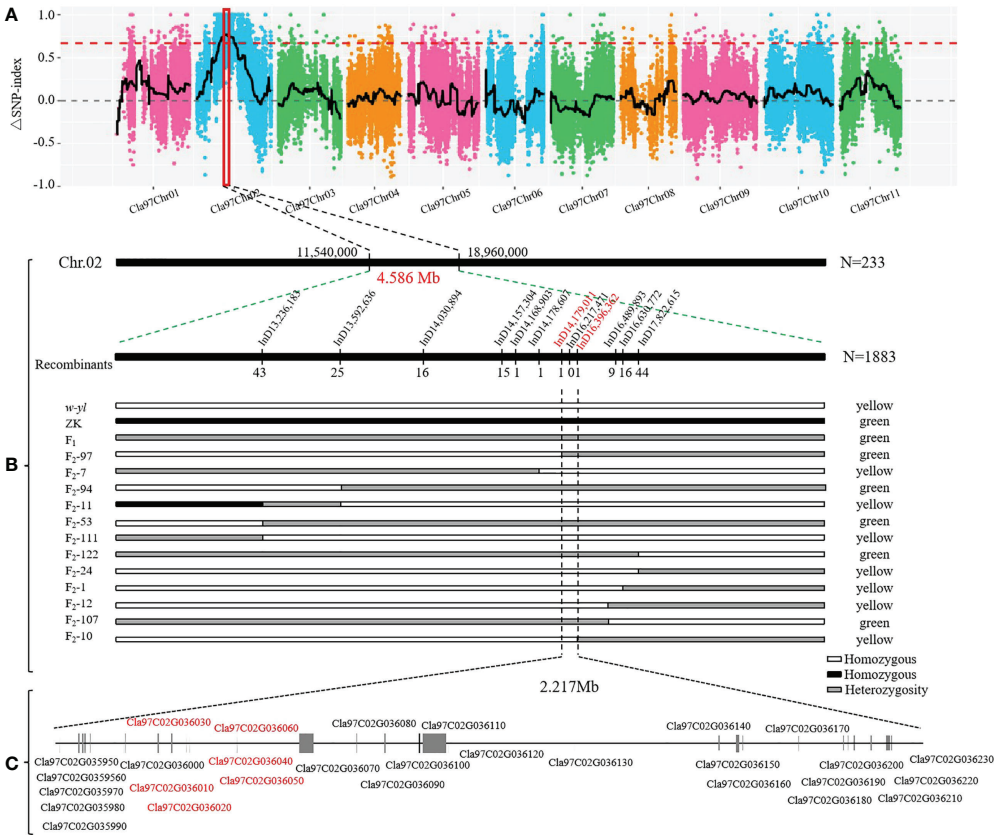

FIGURE 6
Location of yellowing gene on watermelon chromosome 2. **(A)** Δ(SNP-index) of watermelon chromosomes. **(B)** The candidate genes was mapped to a 4.586 Mb region between InD14,179,011 and InD16,396,362 on chromosome 2. **(C)** Putative genes in the candidate region based on the watermelon reference genome annotation.

chloroplast ultrastructure of the silenced gene *Cla97C02G030610* (Figure 11B), *Cla97C02G030630* (Figure 11C) and *Cla97C02G030650* (Figure 11D) did not change compared with the blank control (Figure 11A), and all contained normal grana lamella (GL) and plastid globule (PL). However, the ultrastructure of silenced gene *Cla97C02G030640* and *Cla97C02G03060* was significantly changed, and the chloroplast structure may be damaged (red dotted circle area). For silenced gene *Cla97C02G030660* (Figure 11F), there was no PL, and PG stratification was not obvious, appearing in a fuzzy state. Especially for the silenced gene *Cla97C02G030640* (Figure 11D), there was no PL and no obvious PG, speculating that PG was degraded.

Taken together, these results indicated that candidate genes play an important role in causing leaf yellowing, especially *Cla97C02G030640*.

Discussion

There are various types of leaf color mutations, and leaf yellowing was the most common phenomenon (Jin et al., 2021). Plant leaf yellowing mutants, also known as chlorophyll deficiency mutants, are usually caused by the destruction of chlorophyll synthesis or degradation pathways (Yang et al., 2014). At present, yellowing mutants have been found in rice (Zhang et al., 2017), tomato (Yao et al., 2010) and rape (Xiao et al., 2013). In this study, we reported a whole growth period leaf yellowing watermelon material *w-yl* (Figure 1A), which is completely different from the published watermelon leaf color mutant material (Wang et al., 2011; Haileslassie, 2020), and the leaf yellowing characteristics of *w-yl* can be stably inherited. Light can affect plant chloroplast development and chlorophyll metabolism. For example, light intensity is very important for chloroplast formation (Franck et al., 2000), which can change the proportion and content of anthocyanins or chlorophyll or carotenoids by affecting the activity of enzymes related to pigment synthesis or the expression of genes related to photosynthesis, thus causing the color change of leaves, and eventually leading to the formation of leaf color mutants (Xu et al., 2021). In cucumber, the pigment content of the post-green mutant *SC311Y* increased significantly under lower light

TABLE 2 Gene function annotation information in candidate interval.

Gene name	Gene function
Cla97C02G035950	Translator-related TMA7
Cla97C02G035960	BZIP transcription factor, putative (DUF1664)
Cla97C02G035970	lipid-binding serum glycoprotein
Cla97C02G035980	Protein nucleo-fusion transmitter 6, chloroplast/ mitochondria-like isoform X1
Cla97C02G035990	Unknown protein
Cla97C02G036000	L-ascorbate oxidase homolog, Oxidoreductase activity, Cu^{2+} binding
Cla97C02G036010	Unknown protein
Cla97C02G036020	Two component response regulator like protein
Cla97C02G036030	Transmembrane protein, putative
Cla97C02G036040	Protein containing DUF679 domain
Cla97C02G036050	DnaJ homologous subfamily B member 13 like
Cla97C02G036060	Protein Ycf2
Cla97C02G036070	U11/U12 small ribonucleoprotein 65 kDa protein isoform X2
Cla97C02G036080	Unknown protein
Cla97C02G036090	RING-type E3 ubiquitin transferase
Cla97C02G036100	family proteins containing pentapeptide repeats
Cla97C02G036110	Niemann-Pick C1 protein-like isoform X2
Cla97C02G036120	Zinc finger family protein
Cla97C02G036130	Integral hemolysin III-like protein
Cla97C02G036140	Ser/Thr-rich T10 in the DGCR region
Cla97C02G036150	Phosphoglycerate mutagenase family proteins
Cla97C02G036160	SEC1 family transporter SLY1, Oxidoreductase activity, Mg^{2+} binding
Cla97C02G036170	Unknown protein
Cla97C02G036180	Retrotransposon protein, unclassified
Cla97C02G036190	Glycine-rich RNA-binding protein, putative
Cla97C02G036200	Plant UBX domain protein 4
Cla97C02G036210	Calcium-permeable stress-gated cation channel 1
Cla97C02G036220	Acid phosphatase/vanadium-dependent haloperoxidase-related protein
Cla97C02G036230	Core-2/I branch β-1,6-N-acetylglucosamine aminotransferase family proteins

conditions and was vulnerable to light (Zhang et al., 2022). In addition, the synthesis process of chlorophyll is regulated by many enzymes, and its activity is regulated by temperature (Yang et al., 2018). In rice, mutant *tcd9* showed abnormal chloroplasts and fewer thylakoid lamellae in albino mutant seedlings at low temperature, but the mutant showed normal green color at high temperature (Jiang et al., 2014). In *Arabidopsis*, a heat-sensitive mutant in *tsl1* is impaired in chloroplast RNA editing at high temperatures, hampering chloroplast development (Sun et al., 2020). However, under high temperature and low temperature, high light intensity and low light intensity, chlorophyll content and carotenoid content of *w-yl* had no significant difference compared with normal temperature and light intensity (Figures 1B–F), which suggesting that the mutant *w-yl* was non-photosensitive and non-temperature sensitive.

Previous study had confirmed that the chloroplast volume, the number of thylakoids and the number of grana lamellae in the leaves of mutant *w-yl* are smaller, which leads to a significant reduction in chlorophyll content (Ren et al., 2019). In fact, leaf yellowing mutations are usually caused by incomplete chloroplast development. For example, the yellow green leaf mutant *ygl8* in rice was caused by chloroplast dysplasia (Kong et al., 2016) The mutation of *ChlI/Chl9*^{pyl3} gene in rice leaded to the formation of *pyl3* mutant with light yellow leaves. which inhibited chlorophyll synthesis, resulting in chloroplast dysplasia and leaf color variation (Hu et al., 2021). In *Brassica napus*, the chloroplast morphology of the leaf yellowing mutant *S28-y* was abnormal, with no complete grana and grana lamellae, resulting in total chlorophyll deficiency (Ge et al., 2022). A large number of studies have shown that chlorophyll is the main factor affecting leaf color phenotype, and leaf color phenotype is closely related to chlorophyll content, and the proportion of photosynthetic pigments in leaves can be directly expressed by the depth of leaf color (Chen et al., 2017; Chen et al., 2018; Su et al., 2020). Chlorophyll precursor material is the intermediate product of chlorophyll synthesis process, any step of which will influence the chlorophyll content (Wang et al., 2009) (Beale, 2005). For example, in rice leaf yellowing mutant *W1*, the process from porphobilinogen to uroporphyrinogen III was blocked, which hindered the synthesis of chlorophyll (Cui et al., 2001). In addition, Kong et al. found that the *YGL8* gene isolated and identified in *ygl8* rice yellow-green leaf mutant can encode Mg-protoIX, which plays an important role in chlorophyll synthesis by affecting the transcription level of this enzyme to change chlorophyll content (Kong et al., 2016). In Ilex × attenuata 'Sunny Foster', the contents of ALA, protoIX, Mg-protoIX and pchlide in green-turned leaves were significantly increased, and the chlorophyll content was also significantly higher than that in normal leaves (Huang et al., 2021). Similarly, in *Camellia sinensis* cv. Baiye1, the contents of ALA, protoIX, Mg-protoIX and pchlide were higher in green leaves, and the chlorophyll content was also significantly higher than that in albino leaves (Wang et al., 2008). Similar results were obtained in this study, such as the contents of ALA, protoIX, Mg-ProtoIX and pchlide in *w-yl* were significantly lower than those in normal leaves ZK, indicating that the low chlorophyll content in *w-yl* may be due to the low content of chlorophyll precursors.

There are many kinds of leaf color mutations, and the genetic rules of different mutations vary greatly, which may be nuclear inheritance or cytoplasmic inheritance. For example, rice (Sun et al., 2017), maize (Wang et al., 2018) wheat (Jiang, 2018), cucumber (Gao et al., 2016), rape (Wang, 2014), tomato

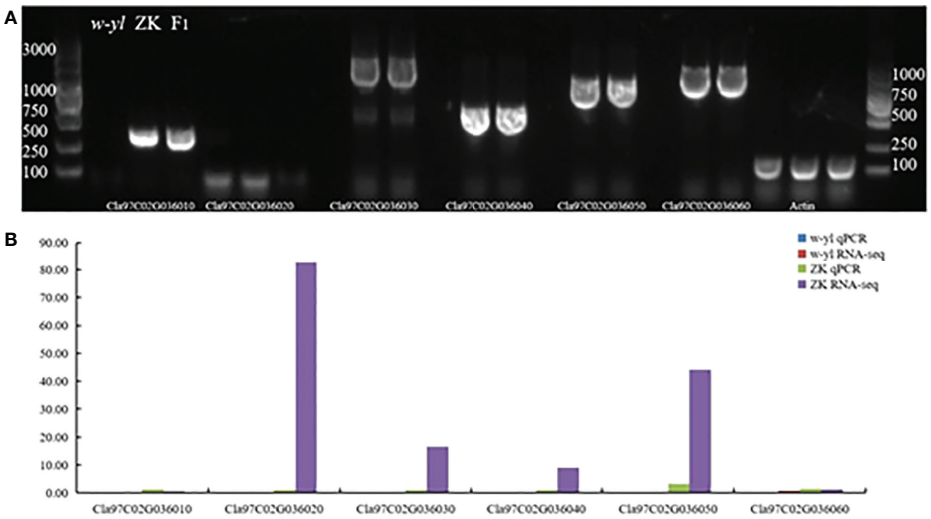

FIGURE 7
Amplification of candidate genes *Cla97C02G036010, Cla97C02G036020, Cla97C02G036030, Cla97C02G036040, Cla97C02G036050* and *Cla97C02G036060*. **(A)** Agarose gel electrophoresis analysis of candidate genes. **(B)** RNA-seq and qPCR analysis of candidate genes.

(Guo, 2017) and cabbage (Zhang, 2017) are controlled by single or two pairs of recessive nuclear genes. In watermelon, Zhang et al. (1996) proved that albino leaf color mutation was controlled by a pair of recessive alleles (*jaja*). Provvidenti (1994) found that the watermelon leaf color mottle mutation was controlled by a pair of recessive genes (*slv*), and the F_2 population showed a normal:mottled separation ratio of 3:1. Rhodes (1986) found that the post-green mutation was controlled by a recessive gene (*dgdg*). The data in this study indicated that *w-yl* is controlled by a pair of recessive nuclear genes. However, the results of mapping indicated that *w-yl* may have DNA fragment deletion compared to ZK, resulting in *Cla97C02G036010*, *Cla97C02G036030*, *Cla97C02G036040*, *Cla97C02G036050* and part of *Cla97C02G036060* in the interval between InD14,179,011 and InD16,396,362 loss the gene function. Chloroplast genome gene loss is relatively common in nature (Dong, 2012). Studies have shown that the most frequent microstructural changes in the chloroplast genome are insertions and deletions, and have a bias for deletions (Gao et al., 2010). In angiosperms, *rpl22, rpl23*, *rpl32*,

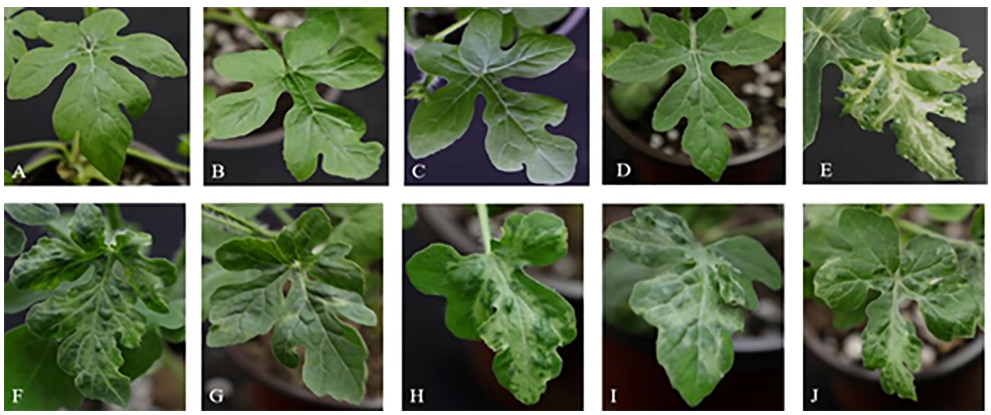

FIGURE 8
Leaf phenotypic analysis of candidate gene silencing. Phenotype of **(A)** blank control, **(B)** water control, **(C)** medium control, **(D)** blank vector control, **(E)** positive control, **(F)** silencing *Cla97C02G036010*, **(G)** silencing *Cla97C02G036030*, **(H)** silencing *Cla97C02G036040*, **(I)** silencing *Cla97C02G036050*, **(J)** silencing *Cla97C02G036060*.

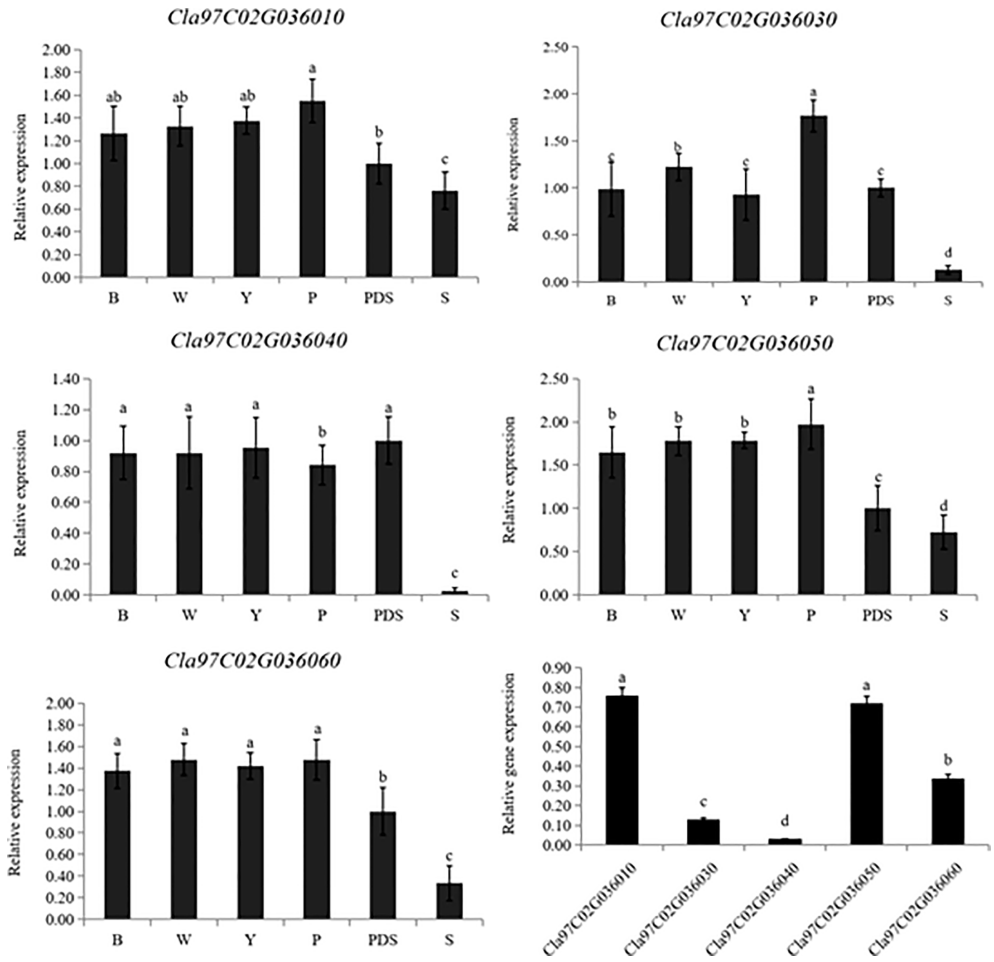

FIGURE 9
Expression levels of silenced genes. B, W, Y, P, PDS and S represents blank control, water control, YEP medium control, blank vector control, positive control and silenced genes, respectively. Small letters represent significant difference at P<0.05.

rpl33, *rps16*, *accD*, *psaI*, *ycf4*, *ycf1*, *ycf2 and infA* were lost in some taxa. Among them, *ycf1*, *ycf2* and *accD* genes were lost in the whole *Gramineae* (Guisinger et al., 2010) and some species in *Solanaceae* (Bruni et al., 2010).

In this study, the gene *Cla97C02G036060* encoded the protein Ycf2. NAD-malate dehydrogenase contained in the Ycf2/FtsHi complex is a key enzyme for ATP production in chloroplasts or non-photosynthetic plastids in the dark (Kikuchi et al., 2018), and is necessary for photosynthetic growth (Parker et al., 2016). The *Ycf2* gene is the largest plastid gene in angiosperms (Huang et al., 2010). It plays an important unknown function in higher plants and is indispensable (Drescher et al., 2000), which can response to biotic and abiotic stresses in plants (Durante et al., 2009) and improve plant cold tolerance (Bernardi et al., 2015). Gene *Cla97C02G036050* encoded a DnaJ-like B subfamily protein, which is a type of heat shock protein (Sun et al., 2018). Its homologous proteins can increase the activity of phytoene synthase in plastids (Zhou et al., 2015), participate in the process of white body differentiation into chloroplasts under light (Shimada et al., 2007), and protect plant photosystem II under heat stress (Wang and Luthe, 2003). For the gene *Cla97C02G036040*, it encoded a protein that containing the DUF679 domain. DUF (domain of unknown function) refers to a protein family with unknown functional domains, which is involved in regulating plant growth and development, plant defense mechanism and plant stress response in plants (Finn et al., 2016; Wang et al., 2022). In *Arabidopsis*, all members of DUF579 family can affect the development of xylan in plant cell wall hemicellulose (Temple et al., 2019), DUF761 is involved in regulating the growth and development of plant vegetative organs (Zhang et al., 2019), DUF642 protein is a specific

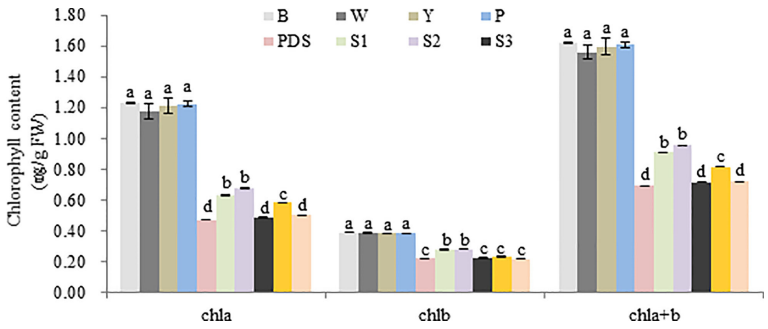

FIGURE 10
Chlorophyll content of different treatment group. B, W, Y, P, PDS, S1, S2, S3, S4,and S5 represents blank control, water control, YEP medium control, blank vector control, positive control, *Cla97C02G036010*, *Cla97C02G036030*, *Cla97C02G036040*, *Cla97C02G036050* and *Cla97C02G036060*, respectively. Small letters represent significant difference at P<0.05.

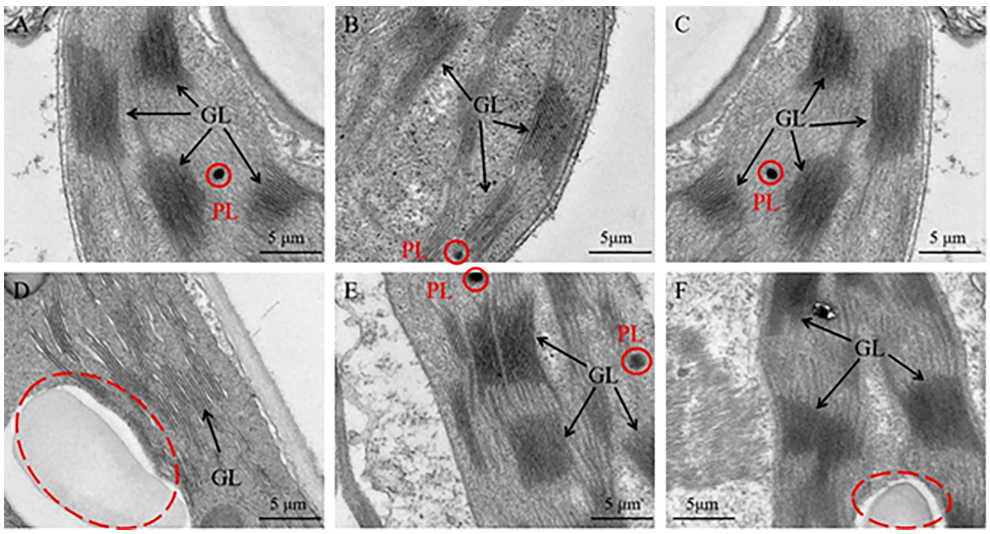

FIGURE 11
Ultrastructure of the chloroplast. **(A)** Chloroplast ultrastructure of blank control, Chloroplast ultrastructure of silencing gene **(B)***Cla97C02G036010*, **(C)** *Cla97C02G036030*, **(D)** *Cla97C02G036040*, **(E)** *Cla97C02G036050* and **(F)** *Cla97C02G036060*, respectively. GL represents grana lamella, PL represents plastoglobuli (red circle). The scale is 5 μm.

protein of seed plants, which is associated with cell wall synthesis (Vázquez-Lobo et al., 2012). In cucurbit crops, there are few studies on DUF domain, mainly focusing on the disease resistance of cucumber (Liu et al., 2010; Qin et al., 2018; Wang et al., 2018).

Data availability statement

The datasets presented in this study can be found inonline repositories. The names of the repository/repositories and accession number(s) can be found below: https://www.ncbi.nlm.nih.gov/, PRJNA872830.

Author contributions

JL, DS, YZ, and GY designed the experiments. YZ, GY, YW, GA, and WL provided experimental methods. YZ and GY performed the research and analyzed the data and wrote the manuscript. JL and DS reviewed the manuscript. All authors contributed to the article and approved the submitted version.

Funding

This research was supported by the National Natural Science Foundation of China (32102395), Natural Science Foundation of Xinjiang Uygur Autonomous Region (2020D01A136), Agricultural Science and Technology Innovation Program (CAAS-ASTIP-2022-ZFRI), the China Agriculture Research System of MOF and MARA (CARS-25), and Joint Key Project of Agricultural Fine Variety in Henan Province (20220100001).

Conflict of interest

The authors declare that the research was conducted in the absence of any commercial or financial relationships that could be construed as a potential conflict of interest.

Publisher's note

Supplementary material

The Supplementary Material for this article can be found online at: https://www.frontiersin.org/articles/10.3389/fpls.2022.1049114/full#supplementary-material

References

Awan, M. A., Konzak, C. F., Rutger, J. N., and Nilan, R. A. (1980). Mutagenic effects of sodium azide in rice. *Crop Sci.* 20, 663–668. doi: 10.2135/cropsci1980.0011183X002000050030x

Beale, S. L. (2005). Green genes gleaned. *Trends Plant Sci.* 10, 309–312. doi: 10.1016/j.tplants.2005.05.005

Bernardi, R., Bartolini, G., Petruccelli, R., Salvini, M., and Durantee, M. (2015). Modulated gene expression during the cold acclimation process in tolerant and sensitive clones of cultivar leccino (*Olea europaea* l.). *Plant Omics* 8, 405–411.

Bruni, I., De Mattia, F., Galimberti, A., Galasso, G., Banfi, E., Casiraghi, M., et al. (2010). Identification of poisonous plants by DNA barcoding approach. *Int. J. Legal Med.* 124, 595–603. doi: 10.1007/s00414-010-0447-3

Chen, T. T., Fu, W. M., Yu, J., Feng, B. H., Li, G. Y., Fu, G. F., et al. (2022). The photosynthetic characteristics of colored rice leaves and their relationship with antioxidant enzyme activities and anthocyanin content. in Chinese agricultural science. *Scientia Agricultura Sin.* 55, 467–478. doi: 10.3864/j.issn.0578-1752.2022.03.004

Chen, L. Y., He, L., Lai, J., He, S., Wu, X., and Zheng, Y. (2017). The variation of chlorophyll biosynthesis and the structure in different color leaves of bambusa multiplex 'Silverstripe'. *J. For. Environ.* 37, 385–391. doi: 10.13324/j.cnki.jfcf.2017.04.001

Chen, K., Li, Z., Cheng, M., Zhao, Y., Zhou, M., and Yang, H. (2018). Chloroplast ultrastructure and chlorophyll fluorescence characteristics of three cultivars of *Pseudosasa japonica*. *Chin. Bull. Bot.* 53, 509–518.DOI: 10.11983/CBB17115

Cui, H. R., Xia, Y. W., and Gao, M. W. (2001). Effects of temperature on leaf color and chlorophyll biosynthesis of rice mutant W1. *J. Nucl. Agric. Sci.* 15, 269–273. doi: 10.3969/j.issn.1000-8551.2001.05.003

Dei, M. (2010). Benzyladenine-induced stimulation of two components of chlorophyII formation in etiolated cucumber cotyledons. *Physiologia Plantarum* 62, 521–526. doi: 10.1111/j.1399-3054.1984.tb02793.x

Dong, W. (2012). *Chloroplast genome evolution of calycanthaceae andhighly variable chloroplast markers development of flowering plants* (Northeast Forestry University: Master).

Dong, H., Fei, G. L., Wu, C. Y., Wu, F. Q., Sun, Y. Y., Chen, M. J., et al. (2013). A rice virescent-yellow leaf mutant reveals new insights into the role and assembly of plastid caseinolytic protease in higher plants. *Plant Physiol.* 162, 1867–1880. doi: 10.1104/pp.113.217604

Drescher, A., Ruf, S., Calsa, T., Carrer, H., and Bock, R. (2000). The two largest chloroplast genome-encoded open reading frames of higher plants are essential genes. *Plant J.* 22, 97–104. doi: 10.1046/j.1365-313x.2000.00722.x

Duan, Y. R., Gao, M. L., Guo, Y., Liang, X. X., Liu, X. J., Xu, H. G., et al. (2022). Map-based cloning and molecular marker development of watermelon fruit shape gene. *Scientia Agricultura Sin.* 55, 2812–2282. doi: 10.3864/j.issn.0578-1752.2022.14.011

Durante, M., Pieretti, M., and Bernardi, R. (2009). Chloropastic ycf2 gene expression in stressed plants. *53° Ital. Soc. Agric. Genet. Annu. Congres* 2, 45.

Finn, R. D., Coggill, P., Eberhardt, R. Y., Eddy, S. R., Mistry, J., Mitchell, A. L., et al. (2016). The pfam protein families database: Towards a more sustainable future. *Nucleic Acids Res.* 44, 279–285. doi: 10.1093/nar/gkv1344

Franck, F., Sperling, U., Frick, G., Pochert, B., Van, C. B., Apel, K., et al. (2000). Regulation of etioplast pigment-protein complexes, inner membrane architecture, and protochlorophyllide alpha chemical heterogeneity by light-dependent NADPH:protochlorophyllide oxidoreductases a and b. *Plant Physiol.* 4, 1678–1696. doi: 10.1104/pp.124.4.1678

Gao, M., Hu, L., Li, Y., and Weng, Y. (2016). The chlorophyll-deficient golden leaf mutation in cucumber is due to a single nucleotide substitution in CsChlI for magnesium chelatase I subunit. *Theor. Appl. Genet.* 129, 1961–1973. doi: 10.1007/s00122-016-2752-9

Gao, P., Liu, S., Cui, H. N., Zhang, T. F., Wang, X. Z., Liu, H. Y., et al. (2020). Research progress of melon genomics,functional gene mapping and genetic engineering. *Acta Hortic. Sin.* 47, 1827–1844doi: 10.16420/j.issn.0513-353x.2020-0489.

Gao, L., Su, Y. J., and Wang, T. (2010). Plastid genome sequencing, comparative genomics, and phylogenomics: Current status and prospects. *J. Systematics Evol.* 48, 77–93. doi: 10.1111/j.1759-6831.2010.00071.x

Ge, Y. S., Yang, J., Wang, R. X., Hong, L., Jiang, W. H., Wu, Z. P., et al. (2022). Preliminary research on the green-revertible yellow leaf mutant S28-y in *Brassica napus*. *J. Yangzhou University(Agricultural Life Sci. Edition)* 43, 20–28. doi: 10.16872/j.cnki.1671-4652.2022.02.003

Gothandam, K., Kim, E., Cho, H., and Chung, Y. (2005). OsPPR1, a pentatricopeptide repeat protein of rice is essential for the chloroplast biogenesis. *Plant Mol. Biol.* 58, 421–433. doi: 10.1007/s11103-005-5702-5

Guisinger, M., Chumley, T., Kuehl, J., Boore, J., and Jansen, R. (2010). Implications of the plastid genome sequence of typha (typhaceae, poales) for understanding genome evolution in poaceae. *J. Mol. Evol.* 70, 149–160. doi: 10.1007/s00239-009-9317-3

Guo, L. J. (2017). *Genetic mapping of a variegated leaf (vg) mutant in tomato* (Huazhong Agricultural University: Master).

Guo, S. G., Zhao, S. J., Sun, H. H., Wang, X., Wu, S., Lin, T., et al. (2019). Resequencing of 414 cultivated and wild watermelon accessions identifies selection for fruit quality traits. *Nat. Genet.* 51, 1616–1623. doi: 10.1038/s41588-019-0518-4

Haileslassie, G. K. (2020). *Genetic and molecular mechanisms of delayed green leaf color and short internode length in watermelon (Citrullus lanatus)* (Chinese Academy of Agricultural Sciences).

Hibara, K., Obara, M., Hayashida, E., Ab, E. M., Ishimaru, T., Satoh, H., et al. (2009). The adaxialized leaf1 gene functions in leaf and embryonic pattern formation in rice. *Dev. Biol.* 334, 345–354. doi: 10.1016/j.ydbio.2009.07.042

Hou, Y., Zhu, Z. C., Zhu, N. N., Chen, K. N., Luan, F. S., and Wang, X. Z. (2016). Construction of EMS mutagenesis watermelon mutant library and phenotypic analysis. *Acta Botanica Boreali-Occidentalia Sin.* 36, 2411–2420. doi: 10.7606/j.issn.1000-4025.2016.12.2411

Huang, J. L., Sun, G. L., and Zhang, D. M. (2010). Molecular evolution and phylogeny of the angiosperm *ycf2* gene. *J. Systematics Evol.* 48, 240–248. doi: 10.1111/j.1759-6831.2010.00080.x

Huang, Q., Su, J., Zhou, P., Zhang, Q., and Zhang, M. (2021). Regulation of chlorophyll metabolism during leaf greening period of llex×attenuata 'Sunny foster'. *J. Northeast Forestry Univ.* 49, 51–54. doi: 10.13759/j.cnki.dlxb.2021.11.010

Huang, R., Wang, Y., Wang, P. R., Li, C. M., Xiao, F. L., Chen, N. G., et al. (2017). A single nucleotide mutation of IspFgene involved in the MEP pathway for isoprenoid biosynthesis causes yellow-green leaf phenotype in rice. *Plant Mol. Biol.* 96, 1–12.doi: 10.1007/s11103-017-0668-7

Hu, B. H., Wang, P., Du, A. P., Li, H., Wang, M. X., Bai, Y. L., et al. (2021). Characterization and gene mapping of *pyl3* mutant in rice. *He Nongxuebao (Journal Nucl. Agric. Sciences)* 35, 2696–2703. doi: 10.11869/j.issn.100-8551.2021.12.2696

Jiang, H. B. (2018). *Identification and gene mapping of chlorophyll- deficient mutant b23 in wheat* (Northwest Agriculture & Forestry University: Master).

Jiang, Q., Mei, J., Gong, X., Xu, J. L., Zhang, J. H., Teng, S., et al. (2014). Importance of the rice TCD9 encoding α subunit of chaperonin protein 60 (Cpn60α) for the chloroplast development during the early leaf stage. *Plant Sci.* 56, 400–410. doi: 10.1016/j.plantsci.2013.11.003

Jin, F. L., Chen, L. Q., Zhang, J. L., Wang, J. J., Li, H. Y., Han, Y. H., et al. (2021). Effects of different ilumination intensities on yellow leaf mutant seedlings of broomcorn millet. *J. Shanxi Agric. University(Natural Sci. Edition)* 41, 26–34. doi: 10.13842/j.cnki.issn1671-8151.202104035

Kenneth, J. L., and Thomas, D. S. (2002). Analysis of relative gene expression data using real-time quantitative PCR and the $2^{-\Delta\Delta CT}$ method. *Methods* 25, 402–408. doi: 10.1006/meth.2001.1262

Kikuchi, S., Asakura, Y., Imai, M., Nakahira, Y., Kotani, Y., Hashiguchi, Y., et al. (2018). A Ycf2-FtsHi heteromeric AAA-ATPase complex is required for chloroplast protein import. *Plant Cell* 30, 2677–2703. doi: 10.1105/tpc.18.00357

Kong, W. Y., Yu, X. W., Chen, H. Y., Liu, L. L., Xiao, Y. J., Wang, Y. L., et al. (2016). The catalytic subunit of magnesium-protoporphyrin IX monomethyl ester cyclase forms a chloroplast complex to regulate chlorophyll biosynthesis in rice. *Plant Mol. Biol.* 92, 177–191. doi: 10.1007/s11103-016-0513-4

Lai, Y., Fu, Q. S., Lv, J. C., Zhou, M., He, M., Xu, W. P., et al. (2018). Analysis of physiological characteristics and chloroplast ultrastructure of a new leaf color mutant in melon. *J. Sichuan Agric. Univ.* 36, 372–379. doi: 10.16036/j.issn.1000-2650.2018.03.015

Lee, H. J., Ball, M. D., Parham, R., and Rebeiz, C. A. (1992). Chloroplast biogenesis 65:enzymic conversion of protoporphyrin ix to mg-protoporphyrin ix in a subplastidic membrane fraction of cucumber etiochloroplasts. *Plant Physiol.* 99, 1134–1140. doi: 10.1104/pp.99.3.1134

Li, Y. (2016). *Physiological characteristics and genetic analysis of leaf color mutant in cucumber* (Sichuan Agricultural University).

Li, R. Q., Jiang, M., Huang, J. Z., Møller, I. M., and Shu, Q. Y. (2021b). Mutations of the genomes *uncoupled4* gene cause ros accumulation and repress expression of peroxidase genes in rice. *Front. Plant Sci.* 12, 682453–682453. doi: 10.3389/fpls.2021.682453

Liu, M. (2019). *Construction of a VIGS vector based on cucumber green mottle mosaic virus* (Chinese Academy of Agricultural Sciences: Master).

Liu, J., Tian, H. L., Wang, Y. H., and Guo, A. G. (2010). A novel antibacterial protein gene GNK2-1 in cucumber and its resistance to fusarium wilt. *Botanical J.* 45, 411–418. doi: 10.3969/j.issn.1674-3466.2010.04.003

Li, C., Wang, J. W., Hu, Z. Y., Xia, Y. Y., Huang, Q., Yu, T., et al. (2021a). A valine residue deletion in ZmSig2A, a sigma factor, accounts for a revertible leaf-color mutation in maize. *Crop J.* 9, 1330–1343. doi: 10.1016/j.cj.2021.01.005

Li, S. Z., Yang, W. Z., and Chen, R. M. (2018). An overview on yellow green leaf mutants in rice. *Biotechnol. Bull.* 34, 15–21. doi: 10.13560/j.cnki.biotech.bull.1985.2018-0465

Ma, S. W., and Zhang, L. (1999). Discovery of mutant strains carrying watermelon albino lethal gene. *Chin. watermelon melon* 4, 22. doi: 10.16861/j.cnki.zggc.1999.04.009

Parker, N., Wang, Y., and Meinke, D. (2016). Analysis of *Arabidopsis* accessions hypersensitive to a loss of chloroplast translation. *Plant Physiol.* 172, 1862–1875. doi: 10.1104/pp.16.01291

Provvidenti, R. (1994). Inheritance of a partial chlorophyll deficiency in watermelon activated by low temperatures at the seedling stage. *Horticulture Sci.* 29, 1062–1063. doi: 10.21273/HORTSCI.29.9.1062

Qin, Z. E., Wang, Y. T., Liu, D., Xin, M., and Zhou, X. Y. (2018). CsCBS clone of cucumber and preliminary verification of its resistance to downy mildew and corynebacterium leaf spot. *J. Northeast Agric. Univ.* 49, 39–47. doi: 10.19720/j.cnki.issn.1005-9369.2018.02.005

Rebeizjames, C. A., Mattheis, R., Smith, B. B., Rebeiz, C. C., and Dayton, D. F. (1975). Chloroplast biogenesis: Biosynthesis and accumulation of mg-protoporphyrin IX monoester and longer wavelength metalloporphyrins by greening cotyledons. *Arch. Biochem. Biophysics* 167, 446–465 10.1016/0003-9861(75)90408-7

Ren, Y. C., Zhu, Y. C., Sun, D. X., Deng, Y., An, G. L., Li, W. H., et al. (2019). Physiological characteristic analysis of a leaf-yellowing mutant in watermelon. *J. Fruit Sci.* 37, 565–573. doi: 10.13925/j.cnki.gsxb.20190508

Rhodes, B. (1986). Genes affecting foliage color in watermelon. *J. Heredity* 77, 134–135. doi: 10.1093/oxfordjournals.jhered.a110190

Sakuraba, Y., Rahman, M. L., Cho, S. H., Kim, Y. S., Koh, H. J., Yoo, S. C., et al. (2013). The rice faded green leaf locus encodes protochlorophyllide oxidoreductase b and is essential for chlorophyll synthesis under high light conditions. *Plant J.* 74, 122–133. doi: 10.1111/tpj.12110

Shao, Q. (2013). *Characterization and proteomics of a novel xantha mutant in muskmelon* (Northeast Agricultural University).

Shao, Q., Yu, Z. Y., Li, X. G., Li, W., and Gao, Y. (2013). Studies on internal physiological and biochemical changes of xantha mutant in melon leaves. *China Vegetables* 14, 59–65. doi: 10.3969/j.issn.1000-6346.2013.14.012

Shimada, H., Mochizuki, M., Ogura, K., Froehlich, J. E., Osteryoung, K. W., Shirano, Y., et al. (2007). *Arabidopsis* cotyledon-specific chloroplast biogenesis factor CYO1 is a protein disulfide isomerase. *Plant Cell* 19, 3157–3169. doi: 10.1105/tpc.107.051714

Sugliani, M., Abdelkefi, H., Ke, H., Bouveret, E., Robaglia, C., Caffarri, S., et al. (2016). An ancient bacterial signaling pathway regulates chloroplast function to influence growth and development in *Arabidopsis*. *Plant Cell* 28, 661–679. doi: 10.1105/tpc.16.00045

Sun, L., Lin, T., Wang, Y., Niu, M., Hu, T., Liu, S., et al. (2017). Phenotypic analysis and gene mapping of a white stripe mutant st13 in rice. *Chin. J. Rice Sci.* 31, 355–363. doi: 10.16819/j.1001-7216.2017.6169

Sun, J. L., Tian, Y. Y., Lian, Q. C., and Liu, J. X. (2020). Mutation of DELAYED GREENING impairs chloroplast RNA editing at elevated ambient temperature in *Arabidopsis*. *J. Genet. Genomics* 47, 200+202–212.

Sun, C. C., Yan, F., and Chen, J. P. (2018). The role of *N. benthamiana* DNA J-like protein in the infection of turnip mosaic virus. *Zhejiang Agric. J.* 30, 2056–2064. doi: 10.3969/j.issn.1004-1524.2018.12.10

Su, J., Shi, W., Yang, Y., Wang, X., Ding, Y., and Lin, S. (2020). Comparison of leaf color and pigment content and observation of leaf structure at different growth stages from six bamboo species. *Scientia Silvae Sinicae* 56, 194–203. doi: 10.11707/j.1001-7488.20200720

Tan, J., Zhang, T., Xia, S. S., Yan, M., Li, F. F., Sang, X. C., et al. (2019). Fine mapping of anovel yellowgreen leaf 14 (ygl14) mutant in rice. *Euphytica* 215, 1–11. doi: 10.1007/s10681-019-2424-3

Temple, H., Mortimer, J. C., Tryfona, T., Yu, X., Lopez-Hernandez, F., Sorieul, M., et al. (2019). Two members of the DUF579 family are responsible for arabinogalactan methylation in *Arabidopsis*. *Plant Direct* 3, e00117. doi: 10.1002/pld3.117

Vázquez-Lobo, A., Roujol, D., Zuiga-Sánchez, E., Albenne, C., Piñero, D., Debuen, A. G., et al. (2012). The highly conserved spermatophyte cell wall DUF642 protein family: Phylogeny and first evidence of interaction with cell wall polysaccharides *in vitro*. *Mol. Phylogenet. Evol.* 63, 510–520. doi: 10.1016/j.ympev.2012.02.001

Wang, J. (2014). *Identification seed purity of "shaanyou 803" in brassca napus l. and molecular markersof one gene underlying chlorophiyll-deficit trait in b. juncea* (Northwest Agriculture & Forestry University: Master).

Wang, F., Duan, S., Li, T., Wang, N., and Tao, Y. (2018). Fine mapping and candidate gene analysis of leaf color mutant in maize. *J. Plant Genet. Resour.* 19, 1205–1209. doi: 10.13430/j.cnki.jpgr.20180326001

Wang, X. R., Hu, Q., Du, X. Z., and Feng., S. (2022). Identification of rice DUF642 family genes and their expression analysis under abiotic stress. *J. Hubei Univ. (Natural Sci. Edition)* 44, 14–23. doi: 10.3969/j.issn.1000-2375.2021.00.010

Wang, D., and Luthe, D. S. (2003). Heat sensitivity in a bentgrass variant. failure to accumulate a chloroplast heat shock protein isoform implicated in heat tolerance. *Plant Physiol.* 133, 319–327. doi: 10.1104/pp.102.018309

Wang, J. M., Ma, S. W., Shang, J. L., and Cheng, S. H. (2011). Leaf colour mutants in cucurbits and their research progress. *J. Anhui Agric. Sci.* 39, 16039–16040+16116. doi: 10.3969/j.issn.0517-6611.2011.26.082

Wang, F. C., and Wang, H. B. (1997). A briefing on the new mutant of watermelon "Yellow bud". *Chin. watermelon melon* 3, 15–16.

Wang, J. Y., Wang, Z. P., and Duan, X. K. (2019). Discovery and genetic analysis of yellow markers in melon buds. *China Vegetables* 32, 15–17.

Wang, P. R., Zhang, F. T., Gao, J. X., Sun, X., and Deng, X. (2009). An overview of chlorophyll biosynthesis in higher plants. *Acta Botanica Boreali-Occidentalia Sin.* 29, 629–636. doi: 10.3321/j.issn:1000-4025.2009.03.032

Wang, X. C., Zhao, L., Yao, M., Chen, L., and Yang, Y. (2008). Preliminary study on gene expression differences between normal leaves and albino leaves of anji baicha (*Camellia sinensis* cv.Baiye1). *J. Tea Sci.* 1, 50–55.

Wu, S., Wang, X., Reddy, U., Sun, H., Bao, K., Gao, L., et al. (2019). Genome of 'Charleston gray', the principal American watermelon cultivar, and genetic characterization of 1,365 accessions in the U.S. national plant germplasm system watermelon collection. *Plant Biotechnol. J.* 153, 994–1003. doi: 10.1111/pbi.13136

Xiao, H. G., Yang, H. W., Rao, Y., Yang, B., and Zhu, Y. (2013). Photosynthetic characteristics and chlorophyll fluorescence kinetic parameters analyses of chlorophyll-reduced mutant in *Brassica napus* l. *Acta Agronomica Sin.* 39, 520–529. doi: 10.3724/SP.J.1006.2013.00520

Xiong, L. R., Du, H., Zhang, K. Y., Lv, D., He, H. L., Pan, J. S., et al. (2020). A mutation in CsYL2.1 encoding a plastid isoform of triose phosphate isomerase leads to yellow leaf 2.1 (*yl2.1*) in cucumber (*Cucumis sativus* l.). *Int. J. Mol. Sci.* 22, 322. doi: 10.3390/ijms22010322

Xu, M., Gao, M. L., Guo, Y., Bao, X. P., Liu, X. J., Liu, J. X., et al. (2022). Photosynthetic characteristics of virescent mutant in watermelon. *J. Northwest A F University(Natural Sci. Edition)* 50, 91–96+106. doi: 10.13207/j.cnki.jnwafu.2022.03.012

Xu, J., Guo, Z. X., jiang, X. X., Ahammedd, G. J., and Zhou, Y. H. (2021). Light regulation of horticultural crop nutrient uptake and utilization. *Horticult Plant J.* 5, 367–379. doi: 10.1016/j.hpj.2021.01.005

Yang, Q. S., He, H., Li, H. Y., Tian, H., Zhang, J. J., Zhai, L. G., et al. (2011). NOA1 functions in a temperature-dependent manner to regulate chlorophyll biosynthesis and rubisco formation in rice. *PloS One* 6, e20015. doi: 10.1371/journal.pone.0020015

Yang, J., Shi, S. L., Ji, X. H., Zhao, L. Q., and Xu, C. Q. (2018). Efect of low temperature stres on physiological indexes of eight species color-leafed trees. *Beifang Yuanyi (Northern Horticulture)* 5, 106–110. doi: 10.11937/bfyy.20172469

Yang, C., Zhang, Y. Y., Fang, Z. Y., Liu, Y. M., Yang, L. M., Zhuang, M., et al. (2014). Photosynthetic physiological characteristics and chloroplast ultrastructure of yellow leaf mutant YL-1 in cabbage. *Acta Hortic. Sin.* 41, 1133–1144. doi: 10.16420/j.issn.0513-353x.2014.06.028

Yao, J. G., Zhang, H., Xu, X. Y., Zhang, L. L., and Li, J. F. (2010). Studies on weak light tolerance of tomato leaf color mutant. *China Vegetables* 4, 31–35. doi: CNKI:SUN:ZGSC.0.2010-04-010

Yuan, G. P., Chun, C. P., Peng, L. Z., Huang, Z. J., Huang, T., Yang, H., et al. (2017). A study on the difference of 'Newhall' navel orange and its sport 'Longhuihong' navel orange. *J. Fruit Sci.* 34, 1117–1124. doi: 10.13925/j.cnki.gsxb.20170096

Yuan, Y. H., Fan, J. L., Yang, W. Z., and Chen, R. M. (2022b). Study on photosynthetic characteristics of 3 maize yellow leaf mutants. *Adv. Biotechnol.* 12, 75–82. doi: 10.19586/j.2095-2341.2021.0097

Yuan, G., Sun, D., An, G., Li, W., Si, W., Liu, J., et al. (2022a). Transcriptomic and metabolomic analysis of the effects of exogenous trehalose on salt tolerance in watermelon (*Citrullus lanatus*). *Cells* 11, 2338. doi: 10.3390/cells11152338

Zhang, K. (2017). *Inheritance and gene mapping of a yellow leaf mutant pylm in pakchoi* (Shenyang Agricultural University).

Zhang, H., Li, J. J., Yoo, J. H., Yoo, S. C., Cho, S. H., Koh, H. J., et al. (2006). Rice chlorina-1 and chlorina-9 encode ChlD and ChlI subunits of mg-chelatase, a key enzyme for chlorophyll synthesis and chloroplast development. *Plant Mol. Biol.* 62, 325–337. doi: 10.1007/s11103-006-9024-z

Zhang, X. P., Rhodes, B. B., Baird, W. V., Skorupska, H. T., and Bridges, W. (1996). Development of genic male-sterile watermelon lines with delayed-green seedling marker. *Hortic. Sci.* 31, 123–126. doi: 10.21273/HORTSCI.31.1.123

Zhang, Z. P., Wang, J. Y., Xing, G. M., Li, M. L., and Li, S. (2022). Integrating physiology, genetics, and transcriptome to decipher a new thermo-sensitive and light-sensitive virescent leaf gene mutant in cucumber. *Front. Plant Sci.* 13, 972620–972620. doi: 10.3389/fpls.2022.972620

Zhang, Y., Zhang, F., and Huang, X. Z. (2019). Characterization of an arabidopsis thaliana DUF761-containing protein with a potential role in development and defense responses. *Theor. Exp. Plant Physiol.* 31, 303–316. doi: 10.1007/s40626-019-00146-w

Zhang, T. Y., Zhou, C. L., Liu, X., Sun, A. L., Cao, P. H., Nguye, T., et al. (2017). Phenotypes and gene mapping of a thermo-sensitive yellow leaf mutant of rice. *Acta Agronomica Sin.* 43, 1426–1433. doi: 10.3724/SP.J.1006.2017.01426

Zhou, X., Welsch, R., Yang, Y., Lvarez, D., Riediger, M., Yuan, H., et al. (2015). *Arabidopsis* OR proteins are the major posttranscriptional regulators of phytoene synthase in controlling carotenoid biosynthesis. *Proc. Natl. Acad. Sci. United States America* 112, 3558–3563. DOI: 10.1073/pnas.1420831112

Zhu, H. Y., Zhang, K. G., Song, P. Y., Zhang, Y., Wang, X. J., Hu, J. B., et al. (2019). Genetic analysis and gene mapping of yellow-green leaf in melon(*Cucumis melo* l.). *J. Henan Agric. Univ.* 53, 16–21. doi: 10.16445/j.cnki.1000-2340.20191025.001